Available online at website: https://journal.bcrec.id/index.php/jcerp

Journal of Chemical Engineering Research Progress, 3 (2) 2026, 159-173

Research Article

Self-Strengthening Bio-based Coatings via Autoxidative Cross-linking of Linseed Oil-Derived Surfactants

Ri Myong Kim[1,], Hyon-Tae Pak[2,*], Son Il Hong[1], Song Hun Kang[1], Song Ik Jo[1], Su Jin Ju[1], Yong Hwan Han[1], Il Song Liang[3]**

[1]*Faculty of Polymer Chemical Engineering, Hamhung University of Chemical Engineering, Hamhung, 999092, Democratic People's Republic of Korea*

[2]*Faculty of Chemistry, Kim Il Sung University, Pyongyang, 999093, Democratic People's Republic of Korea*

[3]*Faculty of Printing Engineering, Pyongyang University of Publishing and Printing, Pyongyang 999093, Democratic People's Republic of Korea.*

Received: 25th March 2026; Revised: 20th April 2026; Accepted: 20th April 2026
Available online: 23th April 2026; Published regularly: December 2026

Abstract

A high-performance, bio-based wax emulsion was formulated using surfactants derived from linseed oil—linseed oil sodium soap (LOS) and linseed oil monoglyceride (LOM). Based on their complementary hydrophilic-lipophilic balance (HLB ~18 for LOS, ~5 for LOM), a 50:50 blend was predicted to match the HLB requirement of beeswax (9–12). Experimental optimization confirmed that a 15% beeswax emulsion stabilized by 5% total concentration of this blend exhibited exceptional properties: fine particle size (D[4,3] = 307 nm), high electrostatic stability (ζ = -31.7 mV), and resistance to centrifugation and thermal aging (50 °C, >28 days). The key innovation lies in the dry film performance. Quantitative FTIR analysis revealed a 72% consumption of C=C bonds over 30 days, confirming spontaneous oxidative crosslinking of the surfactants' unsaturated bonds. This crosslinking led to a continuous 59% increase in elastic modulus (255 → 405 MPa) and superior water resistance (0.9% absorption), significantly outperforming films prepared with conventional saturated or synthetic emulsifiers. This work demonstrates that linseed oil-derived surfactants function as dual-purpose agents, effective emulsifiers and latent crosslinkers, providing a novel strategy for sustainable, high-performance coatings that evolve functionally after application. The intrinsic coating properties were established using PET as an inert model substrate to isolate coating performance from substrate effects. The exceptional barrier and mechanical properties of the developed coating remained effective in preliminary evaluations on paper substrates, confirming its potential for sustainable packaging applications where water resistance and mechanical durability are critical.

Keywords: Wax emulsion; Bio-based surfactant; Oxidative crosslinking; Self-strengthening coating; Sustainable packaging

How to Cite: Kim, R. M., Pak, H. T., Hong, S. I., Kang, S. H., Jo, S. I., Ju, S. J., Han, Y. H., Liang, I. S. (2026). Self-Strengthening Bio-based Coatings via Autoxidative Cross-linking of Linseed Oil-Derived Surfactants. *Journal of Chemical Engineering Research Progress*, 3 (2), 159-173 (doi: 10.9767/jcerp.20691)

Permalink/DOI: https://doi.org/10.9767/jcerp.20691

1. Introduction

Waxes are valued across the textiles, leather, packaging, and coatings industries for their exceptional water repellency, gloss, and protective barrier properties [1-5]. Historically, the application of waxes was predominantly achieved by dissolving or dispersing them in volatile organic compounds (VOCs) such as toluene, white spirit, or chlorinated hydrocarbons to form solvent-based polishes and coatings [6-8]. This practice, however, is associated with significant drawbacks: material and disposal costs are increased due to the price of the solvents themselves and the need for specialized equipment to handle flammability and recover vapors; more critically, the emission of VOCs is led to, which contributes to photochemical smog,

* Corresponding Author.
Email: 13555864570@163.com (H.T. Pak)
13555890450@163.com (R.M. Kim)

poses health risks to workers, and causes environmental pollution [9-12].

To circumvent these issues, a decisive shift towards water-based systems has been undergone by the industry, with the preparation of oil-in-water (O/W) wax emulsions emerging as the most viable and environmentally sound alternative [13-17]. The key challenge in formulating these emulsions is considered to be the stabilization of the molten wax droplets in the aqueous phase against coalescence and Ostwald ripening. This is primarily achieved through two mechanistic approaches: (i) the use of surfactants to reduce interfacial tension and provide electrostatic or steric repulsion, and (ii) the use of solid particles (Pickering stabilization) or polymeric stabilizers [18-25]. Among these, surfactant-stabilized emulsions are the most commercially prevalent due to their formulation flexibility and high efficiency. The emulsification process typically involves high-shear homogenization of the molten wax and a heated surfactant solution, followed by controlled cooling to solidify the wax droplets. This method is widely regarded as the most rational and scalable for producing stable, fine wax emulsions [26, 27].

However, a new dependency on emulsifiers is introduced by this solution, which themselves can be a source of concern. Conventional formulations have relied heavily on synthetic, petroleum-derived surfactants like alkylphenol ethoxylates (APEOs), alcohol ethoxylates, and alkyl sulfates (e.g., SDS). While effective stabilizers, these compounds are increasingly criticized for their poor biodegradability, potential eco-toxicity, and non-renewable origins [26-28]. Furthermore, a critical and often neglected drawback of this approach is the singular focus on achieving emulsion stability, with little consideration given to the role of the emulsifier in the final dry film. These inert, synthetic molecules can remain as low molecular weight components within the wax matrix, acting as plasticizers that compromise the film's mechanical integrity, water resistance, and abrasion durability. Essentially, the very ingredient that enables the green, water-based application can become the weak link in the product's final performance [29-31].

A growing body of research has explored the concept of "reactive surfactants" or "surfmers" that participate in crosslinking reactions during film formation, thereby overcoming the limitations of conventional inert emulsifiers [40]. In coating technologies, such surfactants have been investigated primarily for latex systems, where they copolymerize with acrylic or styrene monomers during film drying [47,48]. However, their application in wax-based systems and the use of vegetable oil-derived reactive surfactants remain largely unexplored. Barquero *et al.* recently reported sugar-based surfactants for stabilizing linseed oil-in-water emulsions, focusing on interfacial activity and rheological properties [32]. While valuable, this study focused on emulsification rather than post-application reactivity of the surfactant itself.

Linseed oil, rich in α-linolenic acid (C18:3, ~50-60%), possesses a high degree of unsaturation that is well-documented to undergo autoxidation and form crosslinked networks—a property that has been exploited for centuries in traditional paints and varnishes [41]. This inherent reactivity makes linseed oil an attractive feedstock for synthesizing surfactants with latent crosslinking functionality. Linseed oil sodium soap (LOS), an anionic surfactant, and linseed oil monoglyceride (LOM), a nonionic surfactant, were synthesized from linseed oil through saponification and glycerolysis, respectively. Based on their estimated hydrophilic-lipophilic balance (HLB) values—approximately 18 for LOS (consistent with Davies' group contribution method for C18 fatty acid soaps [42,43] and similar to sodium oleate [44]) and approximately 5 for LOM (calculated by Griffin's method for monoglycerides [42] and comparable to glycerol monooleate [45])—a 50:50 blend was predicted to achieve an effective HLB of approximately 11.5. This value falls within the reported HLB requirement range for beeswax emulsification (9–12) [42], suggesting that the 50:50 blend might provide optimal emulsion stability.

This study was conducted based on the following hypothesis: surfactants derived from linseed oil (LOS and LOM) can serve dual roles—first as effective emulsifiers for beeswax, with their optimal blend ratio predictable from HLB considerations, and second as latent crosslinkers that undergo spontaneous oxidative crosslinking upon film formation, thereby enhancing the mechanical properties and water resistance of the final coating. The specific objectives of this work are: (i) to synthesize LOS and LOM from linseed oil while preserving their unsaturated bonds; (ii) to experimentally validate the HLB-based prediction by evaluating emulsion stability across a range of LOS:LOM ratios; (iii) to quantitatively demonstrate the occurrence of oxidative crosslinking in the dried films through FTIR analysis; and (iv) to establish the relationship between crosslinking (C=C consumption) and the evolution of film mechanical properties.

This work advances beyond previous research in several key aspects. First, while linseed oil-based soaps have been primarily investigated for cosmetic applications [49] and monoglycerides for polymer synthesis [50], their combined use as emulsifiers for wax systems has not been reported. Second, the potential of the inherent unsaturation in these surfactants to

serve as latent crosslinking sites for post-application film reinforcement has been overlooked. Third, the quantitative relationship between surfactant unsaturation consumption and the evolution of film mechanical properties has not been established. By addressing these gaps, this study demonstrates a transformative strategy where the emulsifier evolves from an inert processing aid to an integral, performance-enhancing component of the final coating.

The present study focuses on establishing the fundamental material properties of the coating on PET films, which serve as a model substrate. PET was selected because its flat, chemically inert surface allows accurate characterization of the coating's intrinsic properties without interference from substrate porosity or surface roughness [31]. The exceptional water resistance (0.9% absorption) and mechanical durability (>400 abrasion cycles) observed on PET films provide a basis for anticipating significant performance improvements on porous paper substrates. Based on this expectation, preliminary coating evaluations on kraft paper were performed in this work to obtain foundational data for future sustainable paper packaging applications.

2. Materials and Method

2.1. Materials

Beeswax (melting point 62-65 °C) was purchased from Sinowax Co., Ltd. (China). Linseed oil (acid value <2 mg KOH/g), sodium hydroxide (NaOH), and glycerol (analytical grade) were obtained from Shanghai Aladdin Biochemical Technology Co., Ltd. (China). Stearic acid (95%), glycerol monostearate (GMS, 95%), Span 60, and Tween 60, used for preparing control samples, were also sourced from Shanghai Aladdin Biochemical Technology Co., Ltd. (China).

2.2. Preparation of Surfactants

2.2.1. Linseed oil sodium soap (LOS)

A 10 M NaOH solution was prepared by slowly adding 13 g of NaOH pellets to 35 mL of cold distilled water in an ice-water bath due to the highly exothermic dissolution. To minimize oxidation of unsaturated bonds, the entire synthesis was performed under continuous nitrogen flow. Linseed oil (100 g) and ethanol (10 mL) were placed in a flask equipped with a reflux condenser and stirred until homogeneous. The mixture was heated to 40–45 °C, and the 10 M NaOH solution was added dropwise while maintaining the temperature. Stirring was continued for 1.5–2 h until a viscous, pale yellow cream formed without visible phase separation.

Hot saturated NaCl solution (100 mL) was added to salt out the soap. The mixture was stirred briefly with mild heating and allowed to settle. The aggregated soap layer was collected and dissolved in 100 mL of hot distilled water, then cooled to precipitate the soap. This washing process was repeated 1–2 times to remove impurities. The purified soap was dried at room temperature and allowed to mature for several days to weeks.

2.2.2. Synthesis of Linseed oil monoglyceride (LOM)

Monoglycerides were synthesized via glycerolysis of linseed oil following established methods [33]. Due to the high unsaturation of linseed oil, the reaction was conducted under continuous nitrogen flow to prevent oxidative degradation. Based on the optimized conditions reported by Igwe and Ogbobe [33], a reaction temperature of 200–220 °C was employed, which is within the range where selective glycerolysis of unsaturated oils occurs while minimizing thermal degradation.

Dehydrated linseed oil (50 g) and glycerol (25 g) were charged into a three-necked flask equipped with a condenser, nitrogen inlet, and thermocouple. Sodium hydroxide (0.25 g, 0.5 wt% of oil) was added as catalyst. The mixture was heated to 200–220 °C with constant stirring under nitrogen flow. Reaction progress was monitored by thin-layer chromatography (TLC) at 30 min intervals; completion typically required 1.5–3 h. Water generated during the reaction was continuously removed using a Dean-Stark apparatus. Upon completion, the system was immediately cooled to 90–100°C to terminate the reaction.

The catalyst was neutralized by dropwise addition of dilute phosphoric acid to pH of 6-7. The product was purified by washing with hot distilled water (50-100 mL, 2-3 times) to remove salts and residual glycerol. The washed product was subsequently dissolved in minimal hot acetone and subjected to gradual cooling crystallization. Monoglycerides were preferentially crystallized due to their lower solubility compared to di- and triglycerides. The resulting monoglyceride crystals were collected by vacuum filtration and dried under nitrogen.

2.3. Preparation of Wax Emulsions

Beeswax emulsions (15% w/w) were prepared using LOS/LOM blends at a total emulsifier concentration of 5% w/w. LOS was first dissolved in a portion of deionized water. The beeswax and remaining water were separately heated to 75–80 °C with constant stirring. After complete melting, the wax phase was stirred at

500 rpm. The LOS solution was added dropwise, followed by LOM in the same manner. The stirring speed was then increased to 1000 rpm, and the aqueous phase was poured in. The coarse emulsion was immediately homogenized at 10,000 rpm for 2–3 min (IKA T25 Digital Ultra-Turrax) until uniform. The emulsion was slowly cooled to room temperature with gentle stirring (200 rpm) to promote uniform wax crystallization. All emulsions were matured for 24 h at room temperature prior to evaluation. Using this method, five formulations with LOS:LOM ratios of 25:75, 40:60, 50:50, 60:40, and 75:25 were prepared (Table 1).

2.4. Characterization of Emulsions

2.4.1. Macroscopic stability

Emulsion stability was evaluated through macroscopic, mechanical, and thermal tests as described below. For the storage stability, emulsion samples in sealed glass bottles were stored at 25 °C and visually inspected daily for signs of creaming, oiling-off, or sedimentation for up to 28 days. For the centrifugation stability, samples were centrifuged at 4000 rpm for 15 min (Centurion Scientific K2015R, UK). The volume of any separated phase was measured, and the emulsification index (EI) was calculated as the percentage of remaining homogeneous emulsion volume relative to the total volume. For the thermal stability, samples were stored at 50 °C (Binder ED, Germany) and inspected daily. The time until first visible phase separation was recorded.

2.4.2. Laser particle size analysis

The volume-weighted mean particle diameter, D [4,3], and the particle size distribution (expressed as the polydispersity index, PDI) were measured using a laser diffraction particle size analyzer (Malvern Mastersizer 3000, UK). To monitor the changes in particle size, measurements were taken at one-week intervals for four weeks after the preparation of the emulsion. Prior to measurement, each sample was gently agitated to ensure homogeneity without causing foam formation or droplet disruption.

Table 1. Emulsifier formulations for stability screening.

Prescription number	LOS: LOM ratio	Estimated HLB values
F_1	25:75	8.25
F_2	40:60	10.2
F_3	50:50	11.5
F_4	60:40	12.8
F_5	75:25	14.75

2.4.3. Zeta potential measurement

The zeta potential of the emulsion droplets was determined using a Zeta potentiometer (Malvern Zetasizer Nano ZS, UK) to assess the electrostatic repulsion between particles and predict colloidal stability. To avoid multiple scattering effects, the emulsion was appropriately diluted with deionized water (approximately 1:100 v/v) until a slightly opaque suspension was achieved. The diluted sample was introduced into a clear disposable zeta cell, and measurements were conducted at 25 °C. The reported value was obtained as the average of at least three consecutive runs.

2.5. Characterization of Dry Films

2.5.1. Preparation of dry films

Three emulsion types were prepared as described in Section 2.4: EXP (50:50 LOS:LOM blend), CTRL-Syn (50:50 Span 60/Tween 60), and CTRL-Sat (50:50 sodium stearate/glycerol monostearate). Each emulsion was cast onto PET sheets using a calibrated applicator to achieve a dry coating weight of 50 g/m². PET film was chosen as a model substrate because its flat, chemically inert surface allows accurate characterization of the coating's intrinsic properties without interference from substrate porosity or surface roughness [1, 31]. The films were conditioned at 25°C and 50% RH for 30 days prior to testing. The visual appearance of the dry films after aging (day 1 and day 15) is shown in Supporting Information Figure S1 and discussed in Section 3.3.

To preliminarily assess the potential for paper packaging applications, the same emulsions were also coated onto kraft paper (basis weight 80 g/m²) at the same coating weight (50 g/m²) using a bar coater. Coated papers were conditioned under identical conditions (25 °C, 50% RH) for 30 days. The results presented in this study are primarily based on PET film measurements, which reflect the intrinsic properties of the coating. Preliminary observations on paper substrates are included as qualitative indicators of potential applicability, with systematic evaluation reserved for future work.

2.5.2. Water contact angle

The surface wettability of the dry films was evaluated by measuring the static water contact angle using a Dataphysics OCA20 instrument (Germany). A deionized water droplet (5 μL in volume) was automatically dispensed onto the

film surface. The contact angle was calculated immediately after droplet deposition using the Young-Laplace fitting method. The measurement was repeated at least five times at different locations on each sample to ensure statistical significance.

2.5.3. Water absorption

The water resistance of the films was quantified through a water absorption test. Pre-weighed dry film samples (W_0) were completely immersed in deionized water at room temperature for 24 hours. Subsequently, the samples were removed, and any surface water was carefully blotted away using a lint-free cloth. The samples were immediately re-weighed to obtain the wet weight (W_W). The percentage of water absorption was calculated using the following equation:

$$Water\ absorption\ (\%) = \frac{W_W - W_0}{W_0} \times 100\% \quad (1)$$

This entire procedure was performed in triplicate for each film formulation to ensure the accuracy and reproducibility of the results.

2.5.4. Abrasion resistance

The mechanical durability of the films against wear was evaluated using a rub tester (GT-KB01, Gester Instruments, China). An abrasive cloth saturated with ethanol was secured to the rubbing finger. A load of 500 g was applied, and the samples were subjected to reciprocal rubbing. The test was continued until visible failure of the film (e.g., wear-through to the substrate) was observed. The number of cycles sustained before failure was recorded as the measure of abrasion resistance.

2.5.5. Mechanical properties (nanoindentation)

Elastic modulus was measured by nanoindentation (Keysight G200, USA) with a Berkovich diamond tip. At least 10 indentations were performed per sample to obtain statistically reliable values. Measurements were conducted on Days 1 and 30 to monitor property evolution indicative of oxidative crosslinking.

2.5.6. Chemical analysis (Fourier-Transform Infrared Spectroscopy - FTIR)

Chemical changes within the films, specifically the consumption of carbon-carbon double bonds (C=C) due to oxidative crosslinking, were monitored by FTIR spectroscopy. Spectra were collected using a Nicolet iS50 spectrometer (Thermo Fisher Scientific, USA) equipped with an ATR accessory. Each spectrum was acquired over 4000–500 cm^{-1}. Measurements were performed on Day 1 and Day 30.

To quantify the extent of crosslinking, the unsaturation index (UI) was calculated from the FTIR spectra. All spectra were analyzed using Origin software (OriginLab, USA). After baseline correction, the integrated areas of the peaks at 3010 cm^{-1} (=C-H stretch of cis-double bonds) and 2854 cm^{-1} (symmetric C-H stretch of methylene groups, internal reference) were obtained using the Integration tool. The unsaturation index was calculated as:

$$UI = \frac{A_{3010}}{A_{2854}} \times 100\% \quad (2)$$

where A_{3010} and A_{2854} are the integrated peak areas.

The percentage of C=C bonds consumed over 30 days was calculated as:

$$(C=C)consumption\ (\%) = \left(1 - \frac{UI_{30}}{UI_1}\right) \times 100\% \quad (3)$$

where UI_1 and UI_{30} are the unsaturation indices on Day 1 and Day 30, respectively. All measurements were performed in triplicate at different locations on each film, and results are reported as mean ± standard deviation.

3. Results and Discussion

3.1. Optimization of Emulsifier Ratio and Emulsion Stability

The stability of beeswax emulsions stabilized with linseed oil-derived surfactants was systematically evaluated through macroscopic, mechanical, thermal, and colloidal characterization. The results, summarized in Table 2, revealed a non-linear relationship between emulsifier ratio and stability, with formulation F_3 (50:50) emerging as the optimal system due to synergistic electrostatic stabilization.

3.1.1. Macroscopic and mechanical stability

Formulations F3 and F4 exhibited excellent mechanical stability, with no precipitation after centrifugation. F2 showed very good stability, while F1 and F5 were significantly unstable. The instability of F5 (high LOS ratio) is attributed to a rigid but mechanically weak interfacial film dominated by ionic surfactant molecules. Under centrifugal force, this brittle film ruptured, causing droplet coalescence and oil separation. Additionally, excess LOS may have compressed the electrical double layer, weakening electrostatic repulsion. Conversely, F1 (high LOM ratio) suffered from insufficient electrostatic repulsion. Although LOM provided effective steric

hindrance, the low surface charge allowed droplets to approach closely, leading to flocculation. The superior performance of F3 and F4 demonstrates a clear synergistic effect: electrostatic repulsion from LOS prevents close approach, while the resilient interfacial film from LOM resists mechanical stress and prevents coalescence [34,35].

3.1.2. Thermal stability

Thermal stability testing at 50 °C revealed that F_3 possessed the longest stability (>28 days), followed by F_2 and F_4, while F_1 and F_5 exhibited the shortest stability periods. Elevated temperature intensifies Brownian motion, increases collision frequency, and reduces the viscosity of the continuous phase. The rapid failure of F_5 again confirmed the fragility of its LOS-dominated interfacial film under thermal stress. The poor performance of F_1 indicated that steric stabilization alone becomes inadequate at higher thermal energies, necessitating a sufficient electrostatic energy barrier to prevent droplet coalescence. The exceptional thermal stability of F_3 was concluded to originate from its balanced stabilization mechanism: electrostatic repulsion provided a high energy barrier, while the tough interfacial film from LOM ensured that droplets did not coalesce upon collision [34].

3.1.3. Particle size distribution and long-term stability

The initial particle size of F_2, F_3, and F_4 was relatively small (<310 nm), but significant differences in long-term (28day) stability were observed. As shown in Figure 1a and 1b, the particle size and polydispersity index of F_3 remained virtually unchanged, indicating its excellent kinetic stability. Moderate growth was

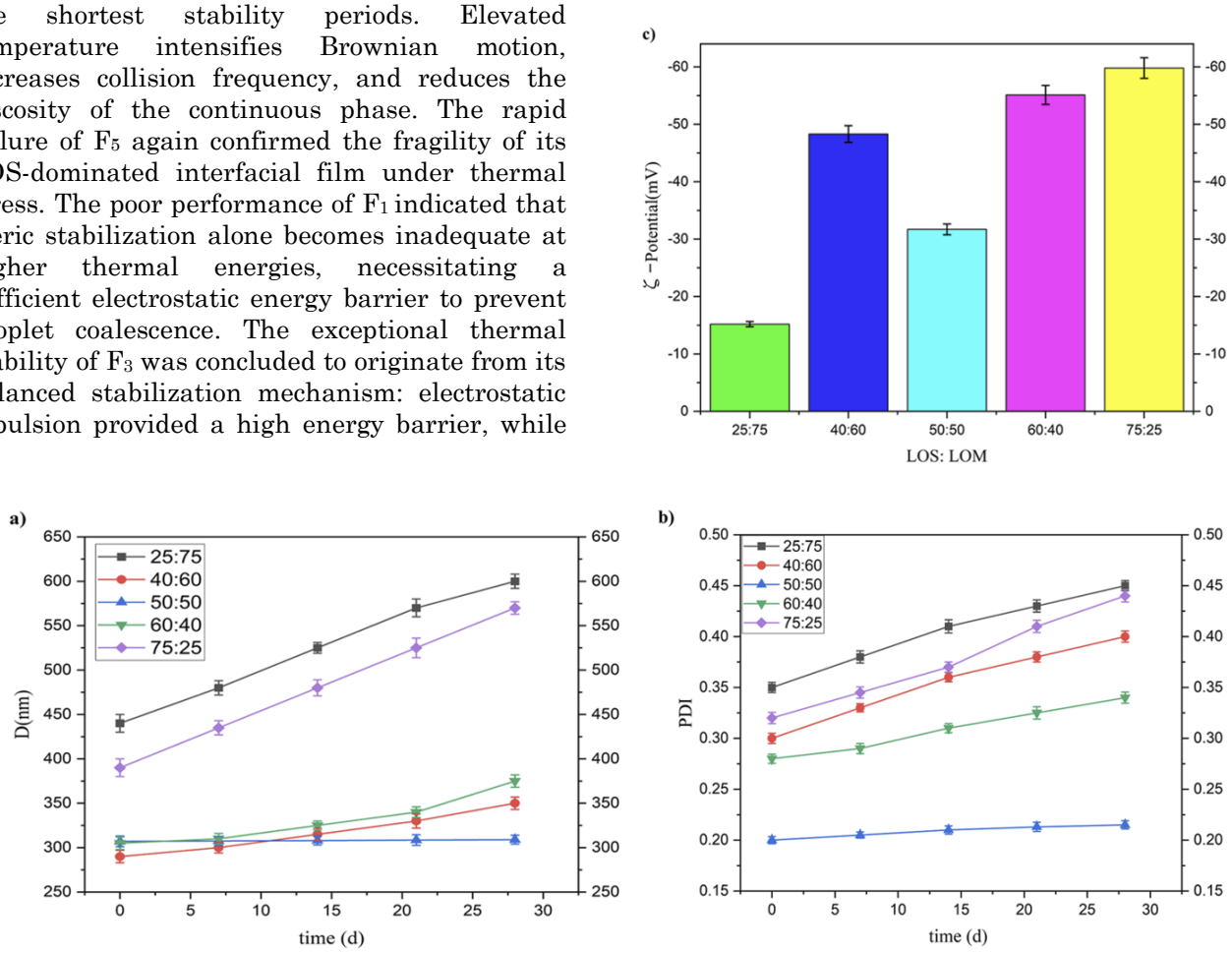

Figure 1. Characteristics of emulsions according to the mixing ratio of emulsifiers: (a) Change in the diameter of the droplet; (b) Change in the polydispersity index; (c) Zeta(ζ) potential.

Table 2. Summary of stability test results for wax emulsion.

Evaluation metrics	F_1 (25:75)	F_2 (40:60)	F_3 (50:50)	F_4 (60:40)	F_5 (75:25)
Macro stability (28 days)	Slight layering	no change	no change	no change	slight sedimentation
Centrifugal precipitation rate (%)	4.2%	0.8%	0%	0.2%	5.5%
Thermal stability (50 ° C, days)	10 d	18 d	>28d	20 d	8 d
Particle size D (4,3) (nm), Day 1	440	290	307	300	390
Particle size D (4,3) (nm), Day 28	600	350	309	375	570
Polydispersity index (PDI), Day 1	0.35	0.32	0.22	0.28	0.3
Zeta potential (mV)	-15.2	-48.3	-31.7	-55.1	-59.8

observed for F_2 and F_4, while the particle size of F_1 and F_5 increased dramatically, suggesting the occurrence of Ostwald ripening and/or aggregation. The stability of F_3 was ascribed to its compact composite interfacial film. This film not only effectively prevented aggregation but also minimized the chemical potential difference between droplets of different sizes, thereby reducing the driving force for Ostwald ripening. Although F_4 exhibited a small initial particle size, its high LOS ratio may have resulted in an overly rigid and hydrophilic interfacial film, which could undergo slight rearrangement during long-term storage, explaining its marginally inferior stability compared to F_3 [36].

3.1.4. Zeta potential and interfacial phenomena

As shown in Figure1c, the zeta potential values followed the order: $|F_5| > |F_4| > |F_2| > |F_3| > |F_1|$. This trend confirmed that a higher LOS ratio generally resulted in a greater negative surface charge. However, a critical finding was that a higher zeta potential did not correlate with improved overall stability. F_5, with the highest potential (-59.8 mV), displayed the poorest stability, demonstrating that excessive electrostatic repulsion is not the sole determinant of stability; the mechanical robustness of the interfacial film is equally crucial. The anomalously high zeta potential of F_2 (-48.3 mV) is explained by the presence of excess, non-adsorbed LOS ions in the aqueous phase, which inflate the measured value without contributing to interfacial cohesion. The zeta potential of F_3 was measured at -31.7 mV. According to DLVO theory, $|\zeta| > 30$ mV provides an excellent electrostatic barrier against aggregation. The potential value of F_3, being just above this threshold and combined with the mechanically robust film provided by LOM, was concluded to create a highly effective "dual-safety" electrosteric stabilization system [34].

3.1.5. HLB-based prediction and experimental confirmation

The effective hydrophilic-lipophilic balance (HLB) of each emulsifier blend was calculated to evaluate whether the experimentally determined optimal formulation (F3) could have been predicted from HLB considerations alone. Based on estimated HLB values of approximately 18 for LOS (consistent with Davies' group contribution method for C18 fatty acid soaps [42, 43] and similar to sodium oleate [44]) and approximately 5 for LOM (calculated by Griffin's method for monoglycerides [42] and comparable to glycerol monooleate [45]), the effective HLB of each blend was determined as the weighted average of the individual surfactant HLB values (Table1). The reported HLB requirement for beeswax emulsification is in the range of 9–12 [42]. A clear correlation was observed between the effective HLB and emulsion stability based on the stability metrics summarized in Table 2.

Formulations with HLB values outside the optimal range exhibited poor stability. F1 (HLB 8.25), with an HLB below the required range, showed phase separation within 10 days at 50°C and a significant increase in particle size over 28 days (from 440 nm to 600 nm). Conversely, F5 (HLB 14.75), with an HLB above the optimal range, failed within 8 days at 50°C and also showed substantial particle size growth (from 390 nm to 570 nm) and poor mechanical stability, evidenced by 5.5% precipitation after centrifugation. In contrast, formulations with HLB values within or near the optimal range all exhibited good to excellent stability. F2 (HLB 10.2), F3 (HLB 11.5), and F4 (HLB 12.8) maintained small particle sizes (<350 nm after 28 days), low polydispersity, and withstood thermal aging at 50°C for at least 18 days (F2, F4) or more than 28 days (F3).

Most notably, F3 (HLB 11.5), which falls closest to the midpoint of the reported optimal HLB range for beeswax, displayed the best overall stability across all metrics. It exhibited the finest initial particle size among the stable formulations (307 nm), the narrowest size distribution (PDI of 0.22), excellent electrostatic stability (ζ = -31.7 mV), and exceptional thermal stability (>28 days at 50°C). Its particle size remained virtually unchanged over the 28-day period (307 nm → 309 nm), indicating outstanding kinetic stability.

This result confirms the validity of the HLB-based prediction made prior to experimentation. Based on the estimated HLB values of LOS (~18) and LOM (~5), a 50:50 blend was predicted to achieve an HLB of approximately 11.5, which falls within the optimal range for beeswax. The experimental data conclusively demonstrate that this prediction was accurate: the 50:50 blend (F3) indeed produced the most stable emulsion among all formulations tested. This agreement between prediction and experiment validates the application of HLB concepts to these bio-based surfactant systems and demonstrates that the optimal formulation could have been identified through rational design rather than trial-and-error alone.

3.1.6. Optimal formulation determination

Although F_3 did not rank first in every individual metric (F_4 had a smaller initial particle size, while F_5 had a higher zeta potential), it was identified as the optimal formulation due to its excellent, balanced, and consistent performance

across all stability tests. This indicates that LOS and LOM achieved optimal synergy at a 50:50 ratio, rather than providing simply additive effects. Its zeta potential provides sufficient electrostatic repulsion, while the steric hindrance of LOM forms a strong interface film, resulting in a synergistic effect where the combined stabilization is greater than the sum of the individual components. The narrow particle size distribution (PDI of 0.22) indicated a uniform emulsion, suitable for industrial production and quality control. Therefore, formulation F3 (LOS:LOM = 50:50) was determined to be the optimal ratio.

3. 2. Comprehensive Analysis of Dry Film Properties

The properties of the dry films derived from the three emulsion types, EXP, CTRL-Sat, and CTRL-Syn, were systematically evaluated after a 30-day aging period. The results, summarized in Table 3, provide conclusive evidence for the unique self-curing mechanism and superior performance of the EXP film, which is comprehensively interpreted below.

3.2.1. Apparent wettability paradox and bulk barrier dominance

As shown in Table 3, Figure 2a and Figure 2b, the EXP film exhibited a moderately hydrophilic surface (82.1°), while both control films showed more hydrophobic surfaces (>100°). This initial discrepancy is attributed to the presence of polar oxidation products (e.g., hydroperoxides, alcohols) at the surface of the EXP film. However, the EXP film demonstrated superior water resistance, as evidenced by its significantly lower water absorption (0.9% vs. 4.0% and 9.0% for the controls).

This apparent contradiction is resolved by considering the film's bulk morphology. The hydrophilic ionic channels formed by LOS likely facilitated oxygen diffusion deep into the film, enabling bulk crosslinking rather than merely surface curing. The resulting highly cross-linked network created a dense, tortuous barrier that physically impeded water penetration. Moreover, the high cross-link density effectively immobilized the hydrophilic groups within the polymer matrix, preventing them from interacting with water molecules despite their presence at the surface. Thus, the superior barrier properties override the influence of surface polarity, demonstrating a decoupling of surface wettability from bulk

Table 3. Comparative properties of dry films after 30 days aging.

Property	EXP	CTRL-Sat	CTRL-Syn
Water Contact Angle (°)	82.1	105	115
Water Absorption (%)	0.9	4.0	9.0
Elastic Modulus, Day 1 (MPa)	255	268	240
Elastic Modulus, Day 30 (MPa)	405	272	242
Abrasion Resistance (cycles)	>400	150	220

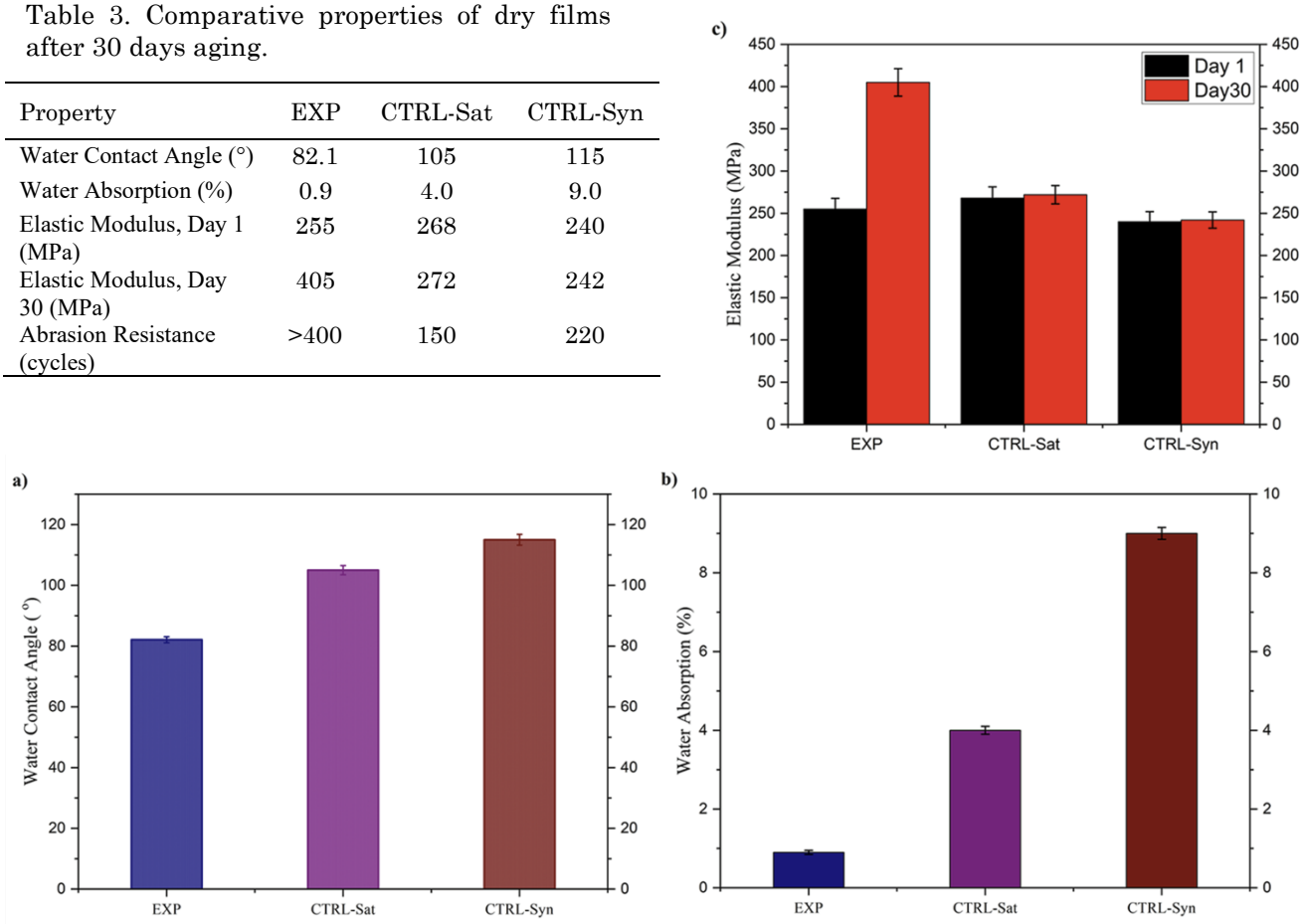

Figure 2. Comparison of water absorption and mechanical properties of dry films: (a) Water Contact Angle; (b) Water absorption; (c) Elastic Modulus.

barrier properties-a recognized effect in cross-linked polymer networks [37].

3.2.2. Mechanistic evolution of mechanical properties

As shown in Figure 2c, exceptional mechanical performance evolution was observed exclusively in the EXP film. Its elastic modulus was increased spontaneously by 59% over 30 days, from 255 MPa to 405 MPa. In contrast, the mechanical properties of both control films remained virtually static. This profound increase is attributed to the formation of covalent carbon-carbon and ether (C-O-C) cross-links, which dramatically increase the crosslink density of the network, a relationship well-established in polymer physics. The most striking improvement was shown in abrasion resistance, where the EXP film sustained more than 400 rub cycles without failure, outperforming both controls by more than 2 times. This is a direct consequence of the high cohesion and mechanical integrity provided by the cross-linked network [38].

3.3. FTIR Spectroscopy Evidence and Comparative Film Performance

The oxidative crosslinking mechanism was confirmed by FTIR spectroscopy through comparative analysis of the EXP film spectra from Day 1 to Day 30, with key changes summarized in Table 4 and Figure 3.

Qualitative FTIR Analysis of the EXP Film: The characteristic peaks for cis-double bonds (C=C stretch at ~1650 cm^{-1}; =C-H stretch at ~3010 cm^{-1}) were significantly diminished over 30 days, confirming their consumption as reactive sites in the crosslinking process [42]. A broad O-H stretch (~3450 cm^{-1}) appeared, indicating hydroperoxide and alcohol formation during autoxidation, while new carbonyl species were detected at ~1710 cm^{-1}, confirming oxidation reactions [51]. Crucially, the C-O stretching region (1200-1000 cm^{-1}) became more intense, signaling the formation of ether (C-O-C) and ester crosslinks—the primary contributors to the three-dimensional network [52]. Additionally, the decrease in the carboxylate ion peak (COO^- at ~1560 cm^{-1}) suggests that LOS was partially protonated

Table 4. FTIR spectral changes indicative of oxidative cross-linking in the EXP film.

Wavenumber (cm^{-1})	Bond Vibration	Change (Day 1 → Day 30)	Interpretation
~3010	=C-H stretch	Disappears/Greatly diminishes	Consumption of cis-double bonds
~1650	C=C stretch	Diminishes/Disappears	Key indicator of cross-linking
~3450	O-H stretch	Becomes more intense and broader	Formation of hydroperoxides and alcohols
~1710	C=O stretch	New peak appears/grows	Formation of carboxylic acids, aldehydes, ketones
~1200-1000	C-O stretch	Becomes more intense and complex	Formation of ether and ester cross-links
~1560	COO^- asym. stretch	Diminishes/Broadens	Protonation of soap and incorporation into network

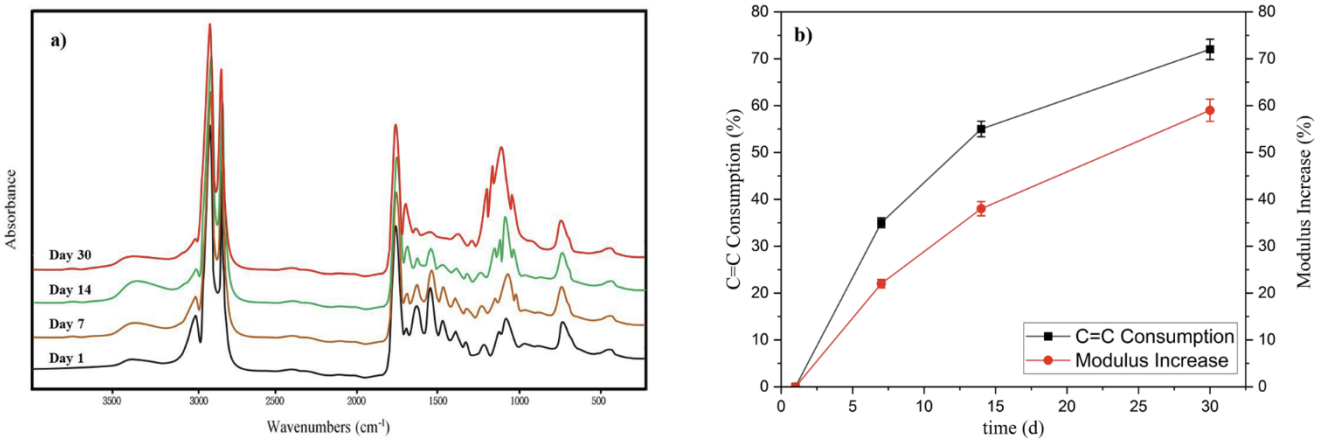

Figure 3. FTIR analysis, C=C consumption, and mechanical property evolution of the EXP film during 30 days of aging. (a) FTIR analysis; (b) C=C consumption and mechanical property evolution.

and incorporated into the network via esterification, transitioning from an emulsifier to a permanent structural component [39].

Quantitative Analysis: To quantify crosslinking, the unsaturation index (UI) was calculated as the ratio of absorbance at 3010 cm^{-1} to that at 2854 cm^{-1} (internal standard) [46]. The extent of C=C bond consumption over 30 days, derived from the unsaturation index (UI), is summarized in Table 5 for all formulations**.** The EXP film showed a dramatic decrease from 0.85 ± 0.03 on Day 1 to 0.24 ± 0.02 on Day 30, corresponding to 72% consumption of C=C bonds—clear evidence of extensive crosslinking. Control formulations exhibited minimal changes: saturated (CTRL-Sat) and synthetic (CTRL-Syn) systems showed no UI change due to the absence of unsaturated bonds, while single-surfactant systems (LOS-only, LOM-only) showed only ~6% consumption. This minor decrease in single-surfactant systems is attributed to surface oxidation without network formation [53].

Multi-Stage Crosslinking and Mechanical Property Development: The relationship between C=C consumption and modulus increase reflects the progressive nature of autoxidative crosslinking [51,52]. Figure 3b presents this relationship for the EXP film based on measurements at 1, 7, 14, and 30 days. The data reveal that the crosslinking process is not uniform over time. During the first 7 days, 35% C=C consumption yielded a 22% modulus increase. Between days 7 and 14, an additional 20% C=C consumption resulted in a further 16% modulus increase. In the final period (days 14-30), 17% additional C=C consumption produced a 21% modulus increase, demonstrating that later-stage crosslinking events contribute more efficiently to mechanical reinforcement. This increasing contribution reflects the progressive formation of the crosslinked network [54]; in the early stage, some consumed unsaturation forms non-network species such as surface oxidation products, while after the gel point, virtually all remaining unsaturation contributes directly to network reinforcement [51,52].

Comparative Film Performance: The FTIR spectra of the control formulations (Figure 4)

Table 5. Comparison of C=C consumption and modulus increase for all formulations.

System	C=C Consumption (%)	Modulus Increase (%)
EXP	72	59
LOS-only	6	2.4
LOM-only	6	2.1
CTRL-Sat	-	1.5
CTRL-Syn	-	0.8

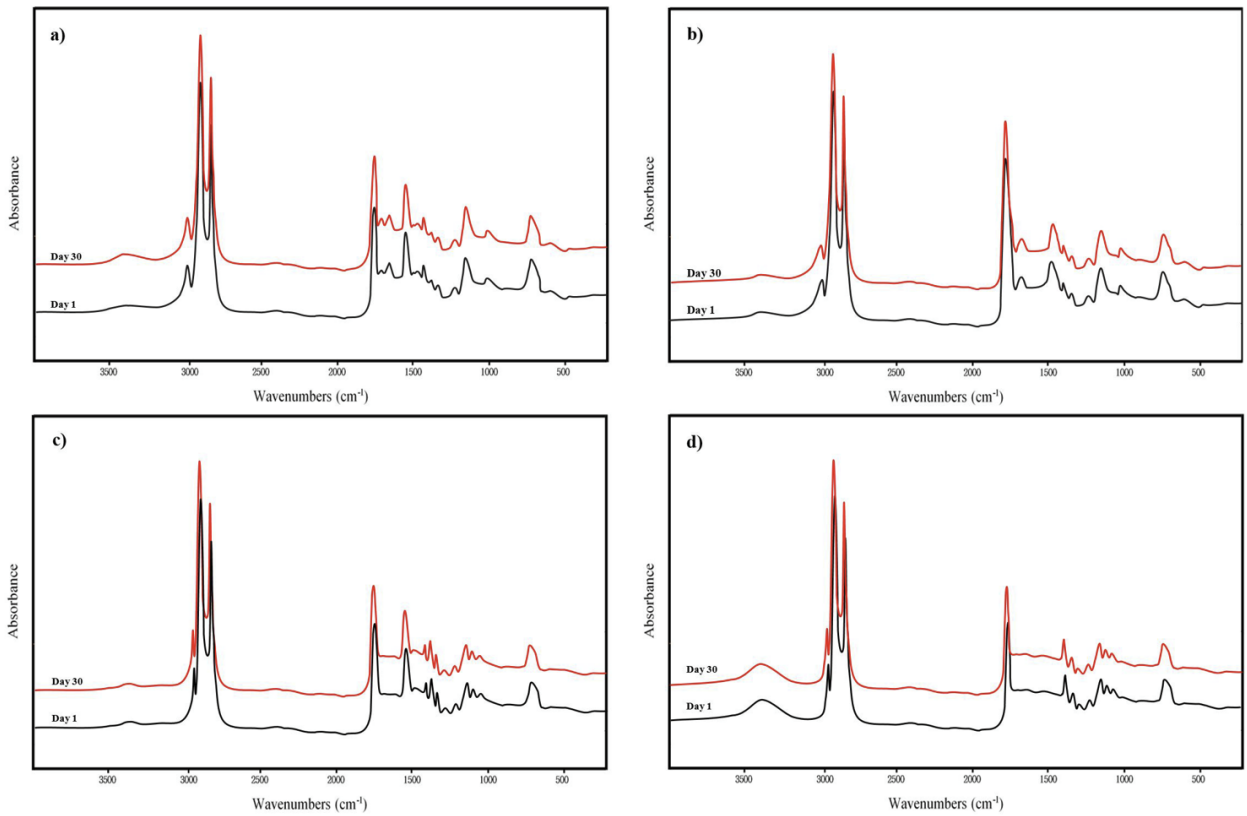

Figure 4. FTIR spectra of control formulations at Day 1 and Day 30. (a) LOS-only film; (b) LOM-only film; (c) CTRL Sat; (d) CTRL Syn.

show no significant changes between Day 1 and Day 30, confirming their chemical inertness. The superiority of the EXP film derives from in-situ oxidative crosslinking, as demonstrated by comparison with control formulations in Table 5. The saturated (CTRL-Sat) and synthetic (CTRL-Syn) systems lack unsaturated bonds entirely, resulting in negligible modulus changes. Their limited mechanical properties arise solely from physical interactions within the wax matrix, in contrast to the EXP film which benefits from covalent network formation.

More significantly, the comparison between EXP and single-surfactant systems (LOS-only, LOM-only) reveals the critical importance of surfactant synergy. Both single-surfactant systems contain unsaturated bonds capable of autoxidation, yet they achieved only ~6% C=C consumption—dramatically lower than the 72% observed in the EXP blend. This six-fold difference demonstrates that the synergistic combination of LOS and LOM is essential for extensive network formation, enabling efficient channeling of oxidative intermediates into crosslinking pathways [35,36]. The negligible modulus increases in single-surfactant systems (2-3%) further confirm that without this synergy, the limited C=C consumption cannot translate into meaningful mechanical reinforcement.

The 72% C=C consumption in the EXP film is consistent with reported extents (60-80%) for autoxidized linseed oil films [53]. The multi-stage relationship between C=C consumption and modulus increase, with later-stage crosslinking events contributing more efficiently, reflects the progressive network development characteristic of autoxidative crosslinking [3,4,8]. The incomplete consumption (72%) is expected due to reduced molecular mobility and steric inaccessibility within the formed network [4,44], with the residual unsaturation (28%) potentially contributing to maintained ductility (15.3% elongation at break) [55].

The absence of C=C consumption in CTRL-Sat and CTRL-Syn confirms these surfactants are chemically inert, serving as negative controls that demonstrate self-strengthening is uniquely attributable to unsaturated bonds in linseed oil-derived surfactants. However, the most compelling evidence for the proposed mechanism comes from the comparison between EXP and single-surfactant systems: both contain unsaturated bonds, yet only their synergistic combination enables the extensive C=C consumption required for substantial mechanical reinforcement [35,36]. These findings establish that the 50:50 LOS:LOM blend creates a reactive system where surfactants evolve from emulsifiers to integral network components, a dual functionality representing a paradigm shift in surfactant design for sustainable, high-performance coatings [29,31].

The macroscopic manifestation of this crosslinking chemistry was directly observable. As shown in Supplementary Figure S1, the EXP film exhibited progressive color darkening from pale yellow on day 1 to yellowish-brown on day 15, whereas control films (CTRL-Syn and CTRL-Sat) showed no visible color change over the same period. This visual evidence qualitatively confirms that autoxidative crosslinking proceeds exclusively in the EXP system, consistent with the quantitative FTIR data presented above.

The multi-stage crosslinking behavior and mechanical reinforcement observed on PET films provide a solid foundation for understanding the coating's intrinsic properties. These results strongly suggest that the EXP coating would perform effectively on paper substrates, where water resistance and mechanical durability are critical requirements for sustainable packaging applications.

3.4. Preliminary Evaluation for Paper Packaging Applications and Future Work

The exceptional water resistance (0.9% absorption) and mechanical durability (>400 abrasion cycles) of the EXP film demonstrated on PET substrates indicate strong potential for paper packaging applications. These properties directly address key requirements for sustainable paper packaging: moisture protection during storage, mechanical integrity during handling and transportation, and compatibility with recycling streams [1,14]. Based on this expectation, the optimal formulation (F3) was applied to kraft paper (basis weight 80 g/m²) at the same coating weight (50 g/m²) for preliminary performance evaluation. Table 6 compares the key characteristics of uncoated paper, control-coated papers, and EXP-coated paper.

The EXP-coated paper exhibited significantly improved water resistance, with a Cobb60 value of 12 g/m², substantially lower than CTRL-Sat (25 g/m²) and CTRL-Syn (18 g/m²) coated papers, as well as uncoated paper (120 g/m²). The water contact angle of 82° on coated paper was consistent with values observed on PET films (82.1°), confirming that the coating's surface properties are preserved on porous substrates. Importantly, the tensile strength of the coated paper increased from 25 MPa to 38 MPa (+52%), demonstrating that the self-strengthening crosslinked network contributes to mechanical reinforcement of the paper substrate. Abrasion resistance also showed a dramatic improvement compared to uncoated paper (<10 cycles), confirming that the excellent intrinsic abrasion resistance of the coating (>400 cycles on PET) is effectively translated to the paper substrate.

These preliminary results demonstrate that the intrinsic properties of the EXP coating, established on PET films, translate effectively to paper substrates, even without optimization of coating process parameters. Table 7 summarizes the key variables, including coating formulation (emulsifier concentration, beeswax content, drier addition), coating process (coating weight, drying conditions), substrate characteristics, and additional performance metrics (WVTR, adhesion, recyclability), to be systematically optimized in future work for commercial paper packaging applications.

These future investigations will provide a comprehensive assessment of the coating's viability for commercial paper packaging applications. The present study establishes the fundamental material platform upon which such applied research can be built.

4. Conclusions

A 50:50 blend of linseed oil sodium soap (LOS) and linseed oil monoglyceride (LOM) at 5% total concentration was identified as the optimal formulation for stabilizing 15% beeswax emulsions. This formulation exhibited fine particle size (307 nm), high electrostatic stability (-31.7 mV), and excellent thermal stability (>28 days at 50 °C). The key innovation of this work lies in the dry film performance. Quantitative FTIR analysis revealed a 72% consumption of C=C bonds over 30 days, confirming spontaneous oxidative crosslinking of the surfactants' unsaturated bonds. This crosslinking led to a continuous 59% increase in elastic modulus (from 255 to 405 MPa) and superior water resistance (0.9% absorption). The EXP film significantly outperformed control formulations in both barrier and mechanical properties. Its water absorption (0.9%) was substantially lower than that of the saturated bio-based (4.0%) and synthetic (9.0%) systems, while its abrasion resistance (>400 cycles) far exceeded the values observed for all control films (150-310 cycles). Single-surfactant systems (LOS-only, LOM-only) showed only ~6% C=C consumption and minimal mechanical changes, demonstrating that the 50:50 blend provides true synergistic benefits. The intrinsic coating properties established on PET films (72% C=C consumption, 59% modulus increase, 0.9% water absorption) remained effective in preliminary evaluations on kraft paper. The EXP-coated paper exhibited excellent water resistance (Cobb60 of 12 g/m²), improved tensile strength (+52%), and markedly enhanced abrasion resistance, confirming its strong potential for sustainable paper packaging applications. Optimization of coating process parameters, including emulsifier concentration, coating weight, drying conditions, and the addition of driers, will be pursued in future work.

Table 6. Preliminary performance of coated kraft paper.

Property	Uncoated Paper	CTRL-Sat Coated	CTRL-Syn Coated	EXP Coated
Water contact angle (°)	0 (instant wetting)	105 ± 3	115 ± 4	82 ± 2
Cobb60 absorption (g/m²)	120 ± 8	25 ± 3	18 ± 2	12 ± 1.5
Tensile strength (MPa)	25 ± 2	27 ± 2	26 ± 2	38 ± 3
Abrasion resistance (cycles)	<10	120 ± 15	180 ± 20	>300

Table 7. Key variables to be optimized in future paper coating studies.

Category	Variable / Property	Objective
Coating formulation	Emulsifier concentration	Maximize barrier and mechanical properties
	Beeswax content	Optimize hydrophobicity
	Drier addition	Accelerate oxidative crosslinking
Coating process	Coating weight	Balance performance and cost
	Drying conditions	Control crosslinking rate
Substrate	Paper type and basis weight	Adapt to target applications
Performance	Water vapor transmission rate (WVTR)	Moisture barrier performance
	Coating adhesion	Mechanical integrity
	Recyclability	End-of-life disposal

This work demonstrates that linseed oil-derived surfactants function as dual-purpose agents, effective emulsifiers that also serve as latent crosslinkers, undergoing spontaneous oxidative crosslinking upon film formation to enhance mechanical properties. This offers a novel strategy for sustainable, high-performance coatings where the emulsifier evolves from an inert processing aid to an integral performance-enhancing component of the final film.

Acknowledgment

The authors declare no acknowledgments.

CRedit Author Statement

Author Contributions: Ri Myong Kim: Conceptualization, Project administration. Hyon-Tae Pak: Writing – original draft, Methodology. Son Il Hong Investigation, Data curation. Song Hun Kang: Validation, Methodology, Investigation, Formal analysis. Song Ik Jo: Validation, Resources, Investigation. Su Jin Ju: Validation, Investigation. Yong Hwan Han: Writing –Original draft writing, Software. Il Song Liang: Visualization, Writing – review & editing. All authors have read and agreed to the published version of the manuscript.

References

[1] Jahangiri, F., Mohanty, A.K., Pal, A.K., Clemmer, R., Gregori, S., Misra, M. (2024). Wax coatings for paper packaging applications: Study of the coating effect on surface, mechanical, and barrier properties. *ACS Environmental Au*, 5, 165-182. DOI: 10.1021/acsenvironau.4c00055.

[2] Pasquier, E., Mattos, B. D., et al. (2022). Multilayers of renewable nanostructured materials with high oxygen and water vapor barriers for food packaging. *ACS Applied Materials & Interfaces*, 14, 30236-30245. DOI: 10.1021/acsami.2c07579.

[3] Zheng, M., Tajvidi, M., Tayeb, A.H., Stark, N.M. (2019). Effects of bentonite on physical, mechanical and barrier properties of cellulose nanofibril hybrid films for packaging applications. *Cellulose*, 26, 5363-5379. DOI: 10.1007/s10570-019-02473-2.

[4] Camargos, C.H.M., Poggi, G., Chelazzi, D., Baglioni, P., Rezende, C.A. (2022). Protective coatings based on cellulose nanofibrils, cellulose nanocrystals, and lignin nanoparticles for the conservation of cellulosic artifacts. *ACS Applied Nano Materials*, 5, 13245-13259. DOI: 10.1021/acsanm.2c02968.

[5] Misra, S. (2024). Coating treatments on jute fabrics for improving their functionality and minimizing the storage losses of grains: A review. *Industrial Crops and Products*, 218, 118742. DOI: 10.1016/j.indcrop.2024.118742.

[6] Wang, S., Zhang, J., Zhang, Y., Wang, L., Sun, Z., Wang, H. (2023). Review on source profiles of volatile organic compounds (VOCs) in typical industries in China. *Atmosphere*, 14, 878. DOI: 10.3390/atmos14050878.

[7] Arshad, M., Shankar, S., Mohanty, A.K., Todd, J., Riddle, R., Van Acker, R., Taylor, G.W., Misra, M. (2024). Improving the barrier and mechanical properties of paper used for packing applications with renewable hydrophobic coatings derived from Camelina Oil. *ACS Omega*, 9, 19786-19795. DOI: 10.1021/acsomega.3c07213.

[8] Nowacka, M., Rybak, K., Wiktor, A., Mika, A., Boruszewski, P., Woch, J., Przybysz, K., Witrowa-Rajchert, D. (2018). The quality and safety of food contact materials–paper and cardboard coated with paraffin emulsion. *Food Control*, 93, 183-190. DOI: 10.1016/j.foodcont.2018.06.011.

[9] Wang, S., Yan, Y., Gao, X., Zhang, H., Cui, Y., He, Q., Wang, Y., Wang, X. (2022). Emission characteristics and health risks of volatile organic compounds (VOCs) measured in a typical recycled rubber plant in China. *International Journal of Environmental Research and Public Health*, 19, 8753. DOI: 10.3390/ijerph19148753.

[10] Tong, R., Zhang, L., Yang, X., Liu, J., Zhou, P., Li, J. (2019). Emission characteristics and probabilistic health risk of volatile organic compounds from solvents in wooden furniture manufacturing. *Journal of Cleaner Production*, 208, 1096-1108. DOI: 10.1016/j.jclepro.2018.10.219.

[11] Huang, H., Wang, Z., Dai, C., Guo, J., Zhang, X. (2022). Volatile organic compounds emission in the rubber products manufacturing processes. *Environmental Research*, 212, 113485. DOI: 10.1016/j.envres.2022.113485.

[12] Sazakli, E., Leotsinidis, M. (2020). Odor nuisance and health risk assessment of VOC emissions from a rendering plant. *Air Quality, Atmosphere & Health*, 14, 301-312. DOI: 10.1007/s11869-020-00935-2.

[13] Sutar, R.S., Wu, X., Latthe, S.S., Shi, B., Xing, R., Liu, S. (2023). Efficient separation of oil-water emulsions: Competent design of superwetting materials for practical applications. *Journal of Environmental Chemical Engineering*, 11, 111299. DOI: 10.1016/j.seppur.2024.127689.

[14] Liu, D., Duan, Y., Wang, S., Gong, M., Dai, H. (2022). Improvement of oil and water barrier properties of food packaging paper by coating with microcrystalline wax emulsion. *Polymers*, 14, 1786. DOI: 10.3390/polym14091786.

[15] Basjari, A., Salehi, A.H., Salamatipour, N. (2020). Bioinspired and green water-repellent finishing of textiles using carnauba wax and layer-by-layer technique. *Journal of the Textile Institute*, 111, 1148-1158. DOI: 10.1080/00405000.2019.1686881.

[16] Janesch, J., Arminger, B., Gindl-Altmutter, W., Hansmann, C. (2020). Superhydrophobic coatings on wood made of plant oil and natural wax. *Progress in Organic Coatings*, 148, 105891. DOI: 10.1016/j.porgcoat.2020.105891.

[17] Clermont-Gallerande, H., Daquin, C., Malvezin, C., Lesbros, C., Nagahiro, C., Bertron, E., Slaim, N., Sanchez, M.A., Pichoutou, O., Guarillof, P. (2022). Substitution of synthetic waxes by plant-based waxes in lipsticks. *OCL*, 29, 19. DOI: 10.1051/ocl/2022010.

[18] Santos, J., Torcato, I.M., Sousa, I. (2017). Assessing differences between Ostwald ripening and coalescence by rheology, laser diffraction and multiple light scattering. *Colloids and Surfaces B: Biointerfaces*, 158, 416-423. DOI: 10.1016/j.colsurfb.2017.08.011.

[19] Prodromidis, P., Katsanidis, E., Biliaderis, C.G., Moschakis, T. (2024). Effect of Tween 20, emulsification temperature and ultrasonication intensity on structured emulsions with monoglycerides. *Food Hydrocolloids*, 147, 109185. DOI: 10.1016/j.foodhyd.2024.109185.

[20] Ma, Q., McClements, D.J., Lu, W. (2023). Water droplets tailored as wax crystal carriers to mitigate wax deposition of emulsion. *ACS Omega*, 8, 7546-7554. DOI: 10.1021/acsomega.2c06809.

[21] Tang, X.Y., Tong, Y.Y., Zhang, Y.H., Yang, P.J., Wang, C.Y., Liu, J.H. (2025). Study on mechanism of surfactant adsorption at oil–water interface and wettability alteration on oil-wet rock surface. *Molecules*, 30, 2541. DOI: 10.3390/molecules30122541.

[22] Bouhoute, M., Taarji, N., Felipe, L.D., et al. (2021). Microfibrillated cellulose from shells as sustainable solid particles for O/W Pickering emulsions. *Carbohydrate Polymers*, 251, 116990. DOI: 10.1016/j.carbpol.2020.116990.

[23] Wang, C., Fu, X., Tang, C.H., et al. (2017). Octenylsuccinate starch spherulites as a stabilizer for Pickering emulsions. F*ood Chemistry*, 227, 298-304. DOI: 10.1016/j.foodchem.2017.01.097.

[24] Ma, Y.X., Li, M., Chen, Z.D., et al. (2023). Construction of butyric acid modified porous starch for stabilizing Pickering emulsions: encapsulation of paclitaxel. *Food Hydrocolloids*, 142, 108858. DOI: 10.1016/j.foodhyd.2023.108858.

[25] Alehosseini, E., Jafari, S.M., Tabarestani, H.S. (2021). Production of D-limonene-loaded Pickering emulsions stabilized by chitosan nanoparticles. *Food Chemistry*, 354, 129591. DOI: 10.1016/j.foodchem.2021.129591.

[26] Cowan-Ellsberry, C., Belanger, S., Dorn, P., Dyer, S., McAvoy, D., Sanderson, H., Versteeg, D., Ferrer, D., Stanton, K. (2014). Environmental safety of the use of major surfactant classes in North America. *Critical Reviews in Environmental Science and Technology*, 44, 1893-1993. DOI: 10.1080/10739149.2013.803777.

[27] Jardak, K., Drogui, P., Daghrir, R. (2016). Surfactants in aquatic and terrestrial environment: occurrence, behavior, and treatment processes. *Environmental Science and Pollution Research*, 23, 3195-3216. DOI: 10.1007/s11356-015-5803-x.

[28] Puig-Grajales, L., Tan, N.G., van der Zee, F., Razo-Flores, E., Field, J.A. (2000). Anaerobic biodegradability of alkylphenols and fuel oxygenates in the presence of alternative electron acceptors. *Applied Microbiology and Biotechnology*, 54, 692-697. DOI: 10.1007/s002530000429.

[29] Fernandes, N., Simões, L., Dias, D. (2023). Comparison of biodegradability, and toxicity effect of biosurfactants with synthetic surfactants. In: Aslam, R., Mobin, M., Aslam, J., Zehra, S. (Eds.) *Advancements in Biosurfactants Research*. Cham: Springer. pp. 117-136. DOI: 10.1007/978-3-031-21682-4_6.

[30] Wang, F. (2021). Preparation optimization and performance evaluation of waterborne epoxy resin for roads. *Advances in Civil Engineering Materials*, 10, 34-46. DOI: 10.1520/ACE104034.

[31] Pérez-Gago, M.B., Krochta, J.M. (2001). Lipid particle size effect on water vapor permeability and mechanical properties of whey protein/beeswax emulsion films. *Journal of Agricultural and Food Chemistry*, 49, 996-1002. DOI: 10.1021/jf000615f.

[32] Barquero, M., Sánchez-García, R.M., Santos, J., Trujillo-Cayado, L.A. (2024). Investigation of linseed oil-in-water nanoemulsions with an ecological surfactant: interfacial activity, stability and rheological enhancements. *Journal of Molecular Liquids*, 415, 126367. DOI: 10.1016/j.molliq.2024.126367.

[33] Igwe, I.O., Ogbobe, O. (2000). Studies on the alcoholysis of some seed oils. *Journal of Applied Polymer Science*, 78(10), 1826-1832. DOI: 10.1002/1097-4628(20001205)78:10<1826::AID-APP150>3.0.CO;2-P.

[34] Liu, Z., Liu, P., Hei, Y., Shi, D., Guo, F., Li, X., Leng, W., Lv, Q., Sun, W. (2024). Synergistic mechanism in anionic/zwitterionic and anionic/nonionic surfactant mixtures on improving the thermal stability of emulsions: an experimental and simulation study. *Chemical Engineering Science*, 289, 119824. DOI: 10.1016/j.ces.2024.119824.

[35] Al-Yousef, Z.A., Almobarky, M.A., Schechter, D.S. (2020). Surfactant and a mixture of surfactant and nanoparticles to stabilize CO2/brine foam, control gas mobility, and enhance oil recovery. *Journal of Petroleum Exploration and Production Technology*, 10, 439-445. DOI: 10.1007/s13202-019-0695-9.

[36] Kundu, P., Agrawal, A., Mateen, H., Mishra, I.M. (2013). Stability of oil-in-water macro-emulsion with anionic surfactant: effect of electrolytes and temperature. *Chemical Engineering Science*, 102, 176-185. DOI: 10.1016/j.ces.2013.07.050.

[37] Rao, X., Zhang, Y., Liu, H. (2022). High-performance and water resistant PVA-based films modified by air plasma treatment. *Membranes*, 12, 249. DOI: 10.3390/membranes12030249.

[38] Forsman, N., Österberg, M., Johansson, L.-S., Kääriäinen, P., Tuure, M., Koivula, H. (2020). Open coating with natural wax particles enables scalable, non-toxic hydrophobation of cellulose-based textiles. *Carbohydrate Polymers*, 227, 115363. DOI: 10.1016/j.carbpol.2019.115363.

[39] Guesmi, R., Benbettaieb, N., Ben Romdhane, M.R., Barhoumi-Slimi, T., Assifaoui, A. (2022). In situ polymerization of linseed oil-based composite film: enhancement of mechanical and water barrier properties by the incorporation of cinnamaldehyde and organoclay. *Molecules*, 27, 8089. DOI: 10.3390/molecules27228089.

[40] Guyot, A. (2002). Recent progress in reactive surfactants in emulsion polymerisation. *Macromolecular Symposia*, 179, 105-132. DOI: 10.1002/1521-3900(200203)179:1<105::AID-MASY105>3.0.CO;2-7.

[41] Van Gorkum, R., Bouwman, E. (2005). The oxidative drying of alkyd paint catalysed by metal complexes. *Coordination Chemistry Reviews*, 249, 1709-1728. DOI: 10.1016/j.ccr.2005.02.002.

[42] Griffin, W.C. (1949). Classification of surface-active agents by HLB. *Journal of the Society of Cosmetic Chemists*, 1, 311-326.

[43] Davies, J.T. (1957). A quantitative kinetic theory of emulsion type. I. Physical chemistry of the emulsifying agent. *Proceedings of the 2nd International Congress of Surface Activity*, 1, 426-438.

[44] ICI Americas Inc. (1984). The HLB System: A Time-Saving Guide to Emulsifier Selection. Wilmington, DE.

[45] Rosen, M.J., Kunjappu, J.T. (2012). Surfactants and Interfacial Phenomena. 4th ed. Hoboken, N.J.: Wiley.

[46] Lazzari, M., Chiantore, O. (1999). Drying and oxidative degradation of linseed oil. *Polymer Degradation and Stability*, 65, 303-313. DOI: 10.1016/S0141-3910(99)00020-8.

[47] El-Aasser, M.S., Tang, J., Wang, X., Daniels, E.S., Dimonie, V.L., Sudol, E.D. (2001). Advances in Emulsion Polymerization For Coatings Applications: Latex Blends And Reactive Surfactants. *Journal of Coatings Technology*, 73(920), 51-63. DOI: 10.1007/BF02698376.

[48] Pereira, A., Trevelyan, P.M.J. (2007). Dynamics of a horizontal thin liquid film in the presence of reactive surfactants. *Physics of Fluids*, 19, 112102. DOI: 10.1063/1.2775938.

[49] 唐振兴, 梁洁玉, 施明珠, 卞继州. (2017). 一种亚麻籽油手工皂及其制备方法 (A linseed oil handmade soap and its preparation method). *Chinese Patent* CN106381242A.

[50] Mosiewicki, M.A., Aranguren, M.I., Borrajo, J. (2005). Mechanical properties of linseed oil monoglyceride maleate/styrene copolymers. *Journal of Applied Polymer Science*, 97(3), 825-836. DOI: 10.1002/app.21790.

[51] Mallégol, J., Gardette, J.L., Lemaire, J. (2000). Long-term behavior of oil-based varnishes and paints. Photo- and thermooxidation of cured linseed oil. *Journal of the American Oil Chemists' Society*, 77(3), 257-263. DOI: 10.1007/s11746-000-0042-4.

[52] Mallégol, J., Lemaire, J., Gardette, J.L. (2000). Drier influence on the curing of linseed oil. *Progress in Organic Coatings*, 39, 107-113. DOI: 10.1016/S0300-9440(00)00126-0.

[53] Juita, Dlugogorski, B.Z., Kennedy, E.M., Mackie, J.C. (2013). Roles of peroxides and unsaturation in spontaneous heating of linseed oil. *Fire Safety Journal*, 61, 108-115. DOI: 10.1016/j.firesaf.2013.07.005.

[54] Flory, P.J. (1953). Principles of Polymer Chemistry. Ithaca, N.Y.: Cornell University Press.

[55] Ashby, M.F. (2010). Materials Selection in Mechanical Design. 4th ed. Oxford: Butterworth-Heinemann.